J Surg Med. 2020;4(1):84-88.
DOI: 10.28982/josam.671514

Research article
Araştırma makalesi

Journal of Surgery and Medicine
e-ISSN=2602-2079

Determination of cancer progression in breast cells by fiber optic bioimpedance spectroscopy system

Fiber optik biyoimpedans spektroskopi sistemi ile meme hücrelerinde kanser gelişiminin belirlenmesi

Tuba Denkçeken [1], Ayşegül Çört [2]

[1] Department of Biophysics, Faculty of Medicine, SANKO University, Gaziantep, Turkey
[2] Department of Biochemistry, Faculty of Medicine, Pamukkale University, Denizli, Turkey

ORCID ID of the author(s)
TD: 0000-0002-4663-5410
AÇ: 0000-0001-8946-7173

Abstract

Aim: It is well established that cancer can be most effectively treated when diagnosed at an early stage. Therefore, development, evaluation, and validation of new biomedical approaches for early detection of cancer and precancerous lesions are important priorities. Our aim was to distinguish low metastatic human breast cells from normal human breast cells using the Fiber Optic Bioimpedance Spectroscopy (FOBIS) system.

Methods: In the FOBIS system we developed, the diameters of the fibers and platinum wires are 50 and 25µm, respectively. The sensitivity of the system to differentiate different cell types was assessed with high metastatic (MDA-MB-231), low metastatic (MCF-7) and normal breast epithelial cells (MCF-10A). Statistical evaluation of data was performed by using Principle Component Analysis (PCA) and Linear Discriminant Analysis (LDA). Spectroscopic data obtained from FOBIS system on suspended human breast cells were evaluated by multivariate statistical analysis to obtain information about the cell type. Fiber optic and bioimpedance methods allow discrimination of different cell types based on their signature. By combining these two techniques, the sensitivity of the system to the differentiation of human breast cells was evaluated.

Results: The discrimination provided the sensitivity of 100% and specificity of 60% in distinguishing MCF-7 from MCF-10A cells.

Conclusion: A highly accurate distinction of breast cancer cells was achieved in cell culture by FOBIS system.

Keywords: Bioimpedance, Breast, Cell distinguish, Fiber optic, Spectroscopy

Öz

Amaç: Kanserin erken evrede teşhis edildiğinde en etkili şekilde tedavi edilebileceği iyi bilinmektedir. Bu nedenle, kanserin ve prekanseröz lezyonların erken tespiti için yeni biyomedikal yaklaşımların geliştirilmesi, değerlendirilmesi ve validasyonu önemli bir önceliktir. Amacımız, Fiber Optik Biyoimpedans Spektroskopisi (FOBIS) sistemini kullanarak düşük metastatik insan meme hücrelerini normal insan meme hücrelerinden ayırt etmekti.

Yöntemler: FOBİS sisteminde 50µm çaplı fiberler ve 25µm çaplı platin teller kullanılmıştır. Sistemin farklı hücre tiplerini ayırt etme duyarlılığı yüksek metastatik (MDA-MB-231), düşük metastatik (MCF-7) ve normal meme epitel hücreleri (MCF-10A) için hesaplanmıştır. Verilerin istatistiksel değerlendirmesi Temel Bileşenler Analizi (TBA) ve Doğrusal Ayırım Analizi (DAA) ile yapılmıştır. İnsan meme hücre kültürlerinde FOBİS sistemi ile elde edilen spektroskopik veriler, çok değişkenli istatistiksel analiz ile değerlendirilerek hücre tipi hakkında bilgi elde edilmiştir. Fiber optik ve biyoimpedans yöntemlerinden elde edilen spektroskopik veriler ile farklı hücre tipleri ayırt edilebilmektedir. Bu iki tekniğin birleştirilmesi ile sistemin insan meme hücrelerinin farklılaşmasına duyarlılığı test edilmiştir.

Bulgular: Buna göre %100 duyarlılık ve %60 seçicilik ile MCF-7 hücreleri MCF-10A hücrelerinden ayırt edilmiştir.

Sonuç: FOBİS sistemi ile hücre kültüründe meme kanseri hücreleri yüksek duyarlılıkla ayırt edilmiştir.

Anahtar kelimeler: Biyoimpedans, Meme, Hücre ayırımı, Fiber optik, Spektroskopi

Corresponding author/Sorumlu yazar:
Tuba Denkçeken
Address/Adres: SANKO Üniversitesi Tıp Fakültesi Biyofizik Anabilim Dalı, 27090 Gaziantep, Türkiye
e-Mail: tdenkceken@sanko.edu.tr

Ethics Committee Approval: The study is not a study with human participants. There are no experiments on animals. This study does not contain any studies on human participants or animals performed by the authors. There is no identifying information of participants.
Etik Kurul Onayı: Bu çalışma, insan katılımcılarla yapılan bir çalışma değildir. Hayvanlar üzerinde deney yoktur. Bu çalışmada, insan katılımcıları veya yazarlar tarafından gerçekleştirilen hayvanlar üzerinde yapılan hiçbir çalışma yoktur. Katılımcıların tanımlayıcı bilgisi yoktur.

Conflict of Interest: No conflict of interest was declared by the authors.
Çıkar Çatışması: Yazarlar çıkar çatışması bildirmemişlerdir.

Financial Disclosure: This research was funded by The Scientific and Technological Research Council of Turkey (TUBITAK), grant number 115E662.
Finansal Destek: Bu çalışma 115E662 numaralı program kodu ile Türkiye Bilimsel ve Teknolojik Araştırma Kurumu (TÜBİTAK) tarafından desteklenmiştir.

Published: 1/31/2020
Yayın Tarihi: 31.01.2020

How to cite/Atıf için: Denkçeken T, Çört A. Determination of cancer progression in breast cells by fiber optic bioimpedance spectroscopy system. J Surg Med. 2020;4(1):84-88.

Introduction

Probes with different diameters and geometries are designed to determine cancerous tissue in recent studies. Individually, fiber optic and impedance measurements are inadequate to detect precancerous lesions in the tissue. Intracellular ($R_{intracelular}$) fluids, extracellular ($R_{extracellular}$) fluids and ion channels ($R_{membrane}$) in the membrane are represented by resistance while the membrane itself is represented by a capacitor ($C_{membrane}$) in the electrical equivalent circuit model of the cell [1]. When an electrical potential is applied to tissue, the current flows through the intracellular and extracellular spaces at high frequencies and extracellular spaces at low frequencies [2]. The cell acts as an insulator in low frequency, and a conductor in high frequency. Current cannot enter the cell membrane and flows out of the cell at zero frequency. Resistance (R: the resistance of the body fluid) and reactance ($X_C=1/2\pi fC$: the resistance of the cell membrane and tissue interface) are components of impedance (Z), which is calculated for each frequency with the formula: $Z^2=X_C^2+R^2$. Reactance, related to the capacitance, causes the phase shift. This phase shift is defined by the Phase Angle (PA) which is calculated with arctan (X_C/R) [3, 4]. The impedance of the tissue varies with the frequency. The current applied to the tissue flows through extracellular fluid because cell membranes function as capacitors. At higher frequencies, this capacitive effect is lost, after which the current passes through the extracellular and intracellular fluid. Thus, the impedance shows a highly resistant characteristic without the reactive component.

Chromatin structure and mucosal integrity change, and cell volume expands, resulting in a decrease in extracellular space and nucleus growth when cancer develops in the tissue [5]. When malignant tumor cells develop in the tissue, various differentiations occur in the membrane and its contents. These differentiations are high aerobic lactate production, abnormal plasma membrane transitions, decreased cell connection, and new antigen formations. Neoplastic changes in the tissue affect sodium, potassium, and calcium ion ratios inside the cell that causes loss of shape, movement, and intercellular communication disorders. All these changes during cancer progression affect cell physiology and thus lead to changes in the electrical properties of the tissue.

Pathologists use morphological criteria like size, shape, nucleus-cytoplasm ratio and glandular structures of the cell during the diagnosis of the tissue. These structures vary in different types of cancer compared to normal tissue. The photons diffuse inside the tissue and some photons reflect from the surface. When light passes from one medium to another, a part of the energy is reflected from the surface of the medium, while another part passes through. When light enters the tissue, it is scattered from the cell membrane because of this difference. Scattering depends on the morphological structure of the tissue. In optical experiments, backscattered light from the tissue is collected as a spectrum, so diagnostic information is provided about the tissue. Salomon et al. [6] used triple spectroscopy technique, and the differentiation of benign and malignant prostate tissue was found with 75% sensitivity after validation. According to this study, the reason for high sensitivity in the differentiation of cancerous tissue was the addition of electrical impedance to the optic and laser system.

In the present study, we aimed to detect cancerous cell type in human breast cell culture in combination with Principle Component Analysis (PCA) and Linear Discriminant Analysis (LDA).

Materials and methods

FOBIS system consists of fiber optic and bioimpedance spectroscopy (Figure 1). Fiber optic part of the system consists of two fiber cables, and the bioimpedance part, two platinum wires. FOBIS system was used for getting optic and impedance spectral information. Current transferred to the media and information about the conductivity of the media was obtained via the bioimpedance part. Adjacent two fiber cables were used in the fiber optic part. Light sent to the media by the fiber that was connected to the light source, and backscattered light was collected with the other fiber for analysis. Since the diameter (50µm) and the numerical aperture (0.22) of the fibers were small (VIS-NIR low OH, 50-micron bare fiber, Ocean Optics), the backscattered light was detected from the surface of the medium. However, singly this optical information was not enough to detect precancerous lesions. For this reason, we added the bioimpedance part to our system. Electrode placement in bioimpedance measurement techniques affects the penetration depth of the signal. Bioimpedance information is obtained from the media surface with electrodes that are placed close to each other in our study. On the other hand, the signal goes more in-depth as the distance between the electrodes increases [7]. Hence, in the bioimpedance part of the system, the platinum wires were placed close to each other so that the bioimpedance information was obtained from the surface of the medium. These allow the optical and bioimpedance parts of the system to receive information from the same surface area in the medium.

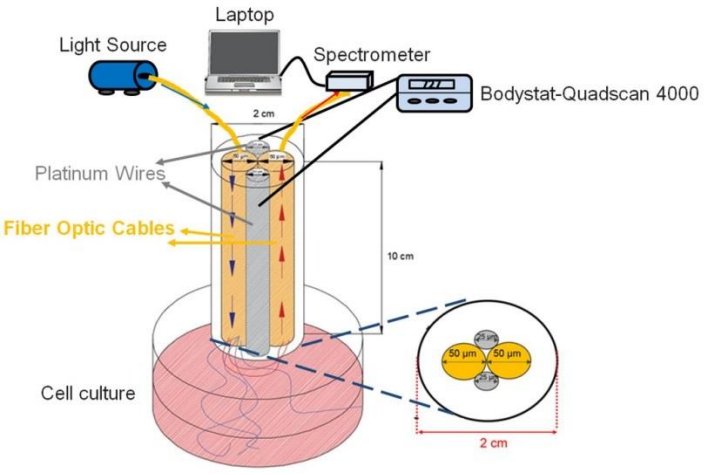

Figure 1: FOBIS system

Design of FOBIS system

Design of Fiber Optic Part: The Fiber Optic part of the system consists of a halogen-tungsten light source (HL-2000 Tungsten Halogen, Ocean Optics), a spectrometer (USB2000+ VIS-NIR Spectrometer, Ocean Optics), a laptop and two fiber optic cables with 50-micron diameter. These two fibers were centered with no distance between them, and all spectral signals were examined by IGOR program (Wavemetrics, Lake Oswego, OR, USA).

Design of Bioimpedance Part: In the second part of the FOBIS system, the 25-micron diameter platinum wires were combined with the optical part as represented in specified geometry in figure 1. To determine whether the platinum wires were in the defined geometry, the signal generator was connected for sending the signal to one end of the platinum wire, and the oscilloscope measured this signal from the other end of the same platinum wire. At the same time, to determine whether the platinum wires were isolated from each other inside the probe, the signal generator was connected for sending the signal to one of the two platinum wires, and the oscilloscope measured this signal from the end of the other platinum wire. In this procedure, the absence of the signal means that isolation was provided. Bioimpedance analyzer (Quadscan 4000, Bodystat Inc.) was connected to the platinum wires to send current to the medium and for impedance measurement. Currents sent in multiple (5, 50, 100 and 200kHz) frequencies and impedance measurements were obtained. Also, resistance, reactance and PA values were recorded at 50kHz frequency.

Calibration procedure of FOBIS system

Bioimpedance Calibration: The frequency versus impedance response of the saline solution is constant, platinum part of the FOBIS probe calibrated by using saline solutions for the known conductivity by using a conductivity meter. The principle of the calibration procedure was to relate the measured transfer impedance to a known uniform conductivity, using a calibration factor or probe constant for each measurement frequency.

Fiber Optic Calibration: Each spectrum was normalized to the integration time, and three spectra were measured for calibration. Firstly, we wanted to eliminate light as much as possible to gather a background spectrum. The tip of the FOBIS probe inserted to a black container which contains pure water and then we measured the back-reflection $R(\lambda)_{bg}$. Secondly, the spectral dispersion of the light source was measured $R(\lambda)_c$ from reflectance standard (Spectralon, Labsphere, Inc.). Confirmation of the calibration was done by observing Mie oscillation from the final spectrum, which was taken from polystyrene microspheres with 2 (0.02) micron diameter. After these calibration measurements, we obtained spectrum from cells, $R(\lambda)_s$ which were corrected by $R(\lambda)=[R(\lambda)_s - R(\lambda)_{bg}]/[R(\lambda)_c - R(\lambda)_{bg}]$.

Cell line

MDA-MB-231, MCF-7, and MCF-10A cells were obtained from the American Type Culture Collection (ATCC). MDA-MB-231 and MCF-7 cells were grown in DMEM supplemented with 4mmol/L L-glutamine and 5% to 10% fetal bovine serum. MCF-10A cells were grown in DMEM/Nut Mix F-12 supplemented with 4mmol/L L-glutamine, 5% serum, 10µg/mL insulin, 20ng/mL epidermal growth factor and 100ng/mL cholera toxins. Cells were chosen with a range of metastatic potential. The average surface area of each cell medium was determined with at least 30 measurements by using an ImageJ (Image Processing and Analysis in Java) open source program. Average surface area of MCF-10A, MCF-7 and MDA-MB-231 cells was calculated as 0.041 (0.019) mm^2, 0.064 (0.017) mm^2 and 0.09 (0.028) mm^2, respectively. Spectroscopic measurements were taken from MDA-MB-231, MCF-7 and MCF-10A cells by FOBIS system to detect the sensitivity to cell type. In order not to adversely affect the sterilization of culture media, FOBIS probe was sterilized with "Cidex-Opa" at each experimental stage.

Statistical analysis

PCA [8,9] followed by LDA [10] was performed to find specific patterns in the wavelength and frequencies for MDA-MB-231, MCF-7 and MCF-10A cells. PCA was used to identify and extract major trends within a given spectral data set. Optic and impedance spectroscopic data matrix "D" (I×C) contains the intensities of scattered light and impedance data from "I" spectra (3); the column number "C" is the number of points for each spectral data (965) and data matrix "D" is separated into several principal components (PCs). The result of PCA is a product of PC scores "S" and PC loadings "F" matrices plus the residue "k": $S= D.F \rightarrow D=S.F'+k=s_1f'_1+s_2f'_2+\ldots s_nf'_n+k$ where D: (IxC) initial data matrix (3x965); S: score $[s_1,s_2,s_3\ldots, s_n]$; F': Eigenvector matrix, loadings, variance; $[f'_1, f'_2, f'_3\ldots, f'_n]$; k: Residual matrix and n is the number of computed PCs. The purpose of PCA is reducing the dimension of observed variables into a relatively smaller number of components while maintaining as much information or variance. Afterward, the acquired components were analyzed by independent-sample t-test for each independent cell types. Statistically significant components were used in LDA to achieve the most precise differentiation of cells. While PCA finds basis vectors corresponding with the direction of the maximal variance of the variables in the data set, LDA searches for those vectors in the underlying space that best discriminates among classes of data and looks for linear combination of variables that best explain the data set [11]. Discrimination is done by setting the variate's weight for each variable to maximize the inter-class variance relative to the intra-class variance of the observation. For confirmation and validation of the analysis, leave-one-out cross-validation (LOOCV) was performed. The areas under the ROC curve (AUC) as well as the sensitivities and specificities for the optimal cut-points are calculated using the discriminant function scores which is obtained by LDA. We used the software package R-Studio Open Source Statistical Language for PCA, LDA and ROC analysis [12,13].

Results

Bioimpedance measurement results

It was found that the impedance value decreases in the suspended metastatic cancer cells in medium (Figure 2a). The reason for this is that the resistance value of the normal breast epithelial cells at lower frequencies is higher than the low and high metastatic resistance values at the same frequencies. The current at low frequencies is exposed to a long resistive pathway around the tight layer of the normal cells. However, the extracellular pathway decreases with the increase of surface area in cancerous cells that causes a decrease in impedance at low frequencies. In the same cell type, impedance was found high due to the strong dielectric properties of the cell membrane and the tissue interface acting as a capacitance in low frequency. However, impedance was found low due to the loss of this capacitive effect of the membrane at high frequencies.

PA values of all cell types were compared, and it was observed that this angle decreased from normal to high

metastasis in cell medium (Figure 2b). According to this finding, different cell types can be detected by using PA values of bioimpedance part of the FOBIS system in the medium.

Fiber optic measurement results

Spectra in the visible wavelength range were acquired from MCF-10A, MCF-7, and MDA-MB-231 cells by using fiber optic part of FOBIS system (Figure 3). At least 16 measurements were collected per cell. A total of 420 spectra were acquired from all cell types, and these spectra were analyzed. As shown in figure 3, the spectral data had different patterns, containing multiple and often overlapping peaks so they turned out to be not very distinct to differentiate cell types from each other. To overcome this limitation, advanced methods of analysis, PCA followed by LDA, were used to differentiate the cell types. In this analysis, firstly we performed a PCA to reduce the number of predictor variables, without much loss of optic and bioimpedance information, used for the differentiation of cell types, which was achieved by first finding the direction having the largest variance (PC1: 59%), and thereafter finding subsequent directions (PC2: 13%, PC3: 11%, PC4: 2%, PC5-15 together gives 1% or less of variance but still contributed significantly). Kruskal-Wallis H-test on all component scores showed that there were one most diagnostically significant (P<0.05) component (PC5) for discriminating cell types. Secondly, the significant component was used as the input variable of LDA. Finally, AUC, as well as the sensitivities and specificities for the optimal cut-points were calculated (Table 1-3).

Table 1: Specificity of FOBIS system for differentiating cell types

Specificity	MCF-10A	MCF-7	MDA-MB-231
MCF-10A	-		
MCF-7	0.60	-	
MDA-MB-231	0.80	0.80	-

Table 2: Sensitivity of FOBIS system for differentiating cell types

Sensitivity	MCF-10A	MCF-7	MDA-MB-231
MCF-10A	-		
MCF-7	1.0	-	
MDA-MB-231	1.0	0.80	-

Table 3: AUC of FOBIS system for differentiating cell types

AUC	MCF-10A	MCF-7	MDA-MB-231
MCF-10A	-		
MCF-7	0.76	-	
MDA-MB-231	0.80	0.76	-

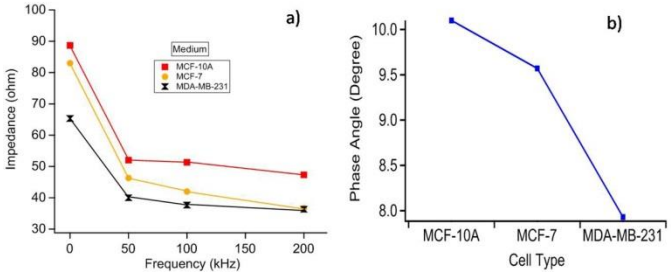

Figure 2: A: MCF-10A, MCF-7 and MDA-MB-231 cells impedance values at multiple frequencies in medium, B: PA values of different cell types in medium

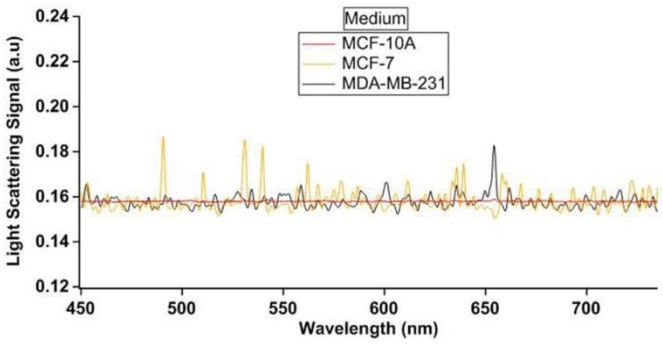

Figure 3: Light scattering signal in the visible range of different cell types in medium

In our study, ROC analysis further confirmed that PCA-LDA based diagnostic algorithms using the all spectral properties of FOBIS system can distinguish low metastatic cancer cells (MCF-7) from normal (MCF-10A) with a sensitivity of 100% and specificity of 60% as seen in figure 4.

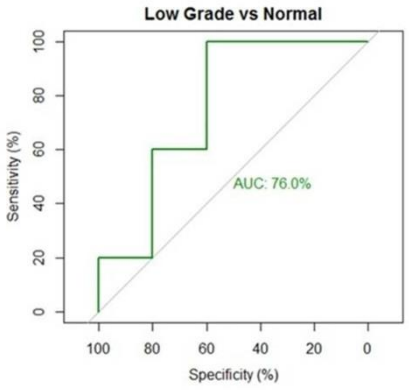

Figure 4: ROC curve comparing low metastatic cancer cell and normal

Discussion

Spectroscopic techniques are quantitative methods which yield more objective results than conventional approaches. In recent years, real-time and noninvasive diagnostic studies have been conducted using optical methods. Molecular and morphological changes in the tissue during the progression of cancer depend on the scatterers of tissue, including nucleus size, nucleus-cytoplasm ratio, and mitochondrial size than scattering and absorption coefficients. These parameters can be correlated with features that are used by pathologists during histological evaluation. The scattering of light from the tissue is more sensitive to changes in the cellular morphology than biochemical changes. Intracellular components such as cell nucleus, mitochondria, lysosomes, Golgi apparatus and the difference in Refractive Index (RI) of cytoplasm causes light scattering in biological tissues [14,15]. In the elastic light scattering, there is no difference between the wavelength of light, which is transmitted to the medium, and the wavelength of the backscattered light. Therefore, there is only the spatial dispersion of light in the medium. In our study, visible wavelength range (450-750 nm) light was used. Due to the small diameter of fibers (50µm) and numerical aperture (0.22), it was improbable that the photons, which were diffused in the medium, were collected by the adjacent optical fibers immediately, entering light into the medium re-collected from the surface of the medium without further deep penetration. With the fiber geometry that was determined in this study, the photons scattered only a few times in the medium were collected, and the sensitivity of the morphological changes in the cell was investigated with the obtained spectral information. With changing the particle size, alteration in the obtained spectra can be explained by Mie theory. According to this theory, the intensity of backscattered light from the medium depends on the scattering phase function (P (θ, λ)) and scattering coefficient $\mu_s(\lambda)$.

The structures in the cell function as biological scatterers. Light scattering occurs in the cell itself, nucleus, structures within organelle and organelle in mammalian cells. These cells are approximately 10-30µm diameter and have 3-10µm nucleus diameter [16]. The length of the mitochondria of these cells is about 1-4µm, and the diameter is around 0.3-0.7µm

[17]. Lysosomes and peroxisomes diameters of these cells are about 0.2-0.5μm [16]. The RI values of these organelles were determined as 1.35-1.36 for extracellular fluid [18], 1.36-1.375 for cytoplasm and 1.38-1.41 for nucleus [19], mitochondria and organelles [20] in the literature. RI value of normal epithelial cells that we studied was found as 1.34 for the growth medium, and RI value of its nucleus was found higher than the cytoplasm [21]. In a study, the RI values of MCF-7 and MDA-MB-231 cells were determined higher than the normal cells. Accordingly, the RI value was determined as 1.37 for normal, 1.401 for MCF-7 and 1.399 for MDA-MB-231 [22]. In our study, due to the difference of RI of the cells in the medium, the light scattering intensity which is obtained from the MCF-10A in which RI is close to the medium was found lower than MDA-MB-231 and MCF-7 which had high RI, consistent with the study in the literature [23].

It has been stated that the capacitive nature of the cell membrane causes the current flow into the surface of cells and the tight junctions act as a "short circuit" which in turn leads to a characteristic drop in impedance at high frequencies [24]. In our study, the impedance value decreased, while cancer progressed in the medium. Over the years, several *in-vitro* and *in-vivo* studies have been conducted to study the dielectric properties of cancerous and non-cancerous breast tissues. For instance, Chauveau et al. [25] conducted an *in-vitro* study of normal and cancerous breast tissues and observed significant differences in their dielectric properties. Surowiec et al. [26] conducted *in-vitro* dielectric studies in the tumor, surrounding the tumor and normal peripheral samples of breast tissues. They found that the tumor tissues had low frequency (100 kHz) conductivity which was higher than the conductivity of normal tissue and lower than that of the surrounding tissue. In another *ex-vivo* study, Fricke et al. [27] measured the parallel capacitance and resistance of the excised samples from the normal and carcinoma breast tissues. They found significantly higher permittivity of the tumor tissue at 20kHz as compared to the normal or benign tissues. PA values decreases from normal to cancer in the medium. The reduction in ionic conductivity and disorientation of cell integrity in cancer progression causes low reactance and low PA. This angle was found high in normal cells where membrane integrity was oriented, and reactance was high. Studies have shown that low PA is associated with the tumor, cell death or decreased cell integrity, but high PA is associated with the healthy cell or cell membrane [4,28-31].

Our results indicate that the FOBIS system can distinguish between MCF-10A and MCF-7 with a sensitivity of 100% and a specificity of 60%, MCF-10A, and MDA-MB-231 with a sensitivity of 100% and a specificity of 80%, MCF-7, and MDA-MB-231 with a sensitivity of 80% and a specificity of 80%. In the previous studies that used fiber optic and bioimpedance systems alone with different geometries, precancerous lesions were detected with low sensitivity [32,33].

Conclusion

It is well established that cancer can be most effectively treated when diagnosed at an early stage. Therefore, development, evaluation, and validation of new biomedical approaches for early detection of cancer and precancerous lesions are important priorities. The FOBIS system that we have developed in this study has been shown to distinguish low metastatic cells from normal cells with 100% sensitivity. Since the measurement takes a long time in this study, this is a constraint when the system is applied to the clinic *ex-vivo* experiments. To overcome this limitation, we are currently developing a scanning system with automation and interface. In this way, through probe tip of FOBIS system that has automation control, the tissue that has large surface area will be scanned in a short time with small steps so any region of the surface area will not be missed. It is planned that the management of the motor step movements, interface and the collection of spectroscopic signals will be performed on the same screen in the computer real time.

References

1. Hodgkin AL, Huxley AF. A quantitative description of membrane current and its application to conduction and excitation in nerve. J Physiol. 1952;117:500-44.
2. Schwan HP. Electrical properties of tissue and cell suspensions. Adv Biol Med Phys. 1957;5:147-209.
3. Lukaski HC. Biological indexes considered in the derivation of the bioelectrical impedance analysis. Am J Clin Nutr. 1996;64:397S-404S.
4. Selberg O, Selberg D. Norms and correlates of bioimpedance phase angle in healthy human subjects, hospitalized patients, and patients with liver cirrhosis. Eur J Appl Physiol. 2002;86:509-16.
5. Farre R, Blondeau K, Clement D, Vicario M, Cardozo L, Vieth M, et al. Evaluation of oesophageal mucosa integrity by the intraluminal impedance technique. Gut. 2011;60:885-92.
6. Salomon G, Hess T, Erbersdobler A, Eichelberg C, Greschner S, Sobchuk AN, et al. The feasibility of prostate cancer detection by triple spectroscopy. Eur Urol. 2009;55:376-83.
7. Grimnes S, Martinsen ØG. Geometrical Analysis in Bioimpedance and Bioelectricity Basics. Academic Press: Oxford; 2015. pp. 141-178.
8. Eriksson L, Andersson PL, Johansson E, Tysklind M. Megavariate analysis of environmental QSAR data. Part II--investigating very complex problem formulations using hierarchical, non-linear and batch-wise extensions of PCA and PLS. Mol Divers. 2006;10:187-205.
9. Abdi H, Williams LJ. Principal component analysis. Wiley Interdiscip Rev Comput Stat. 2010;2:433-59.
10. Fukunaga K. Introduction to Statistical Pattern Recognition. Elsevier Science; 2013.
11. Martinez AM, Kak AC. PCA versus LDA. IEEE T Pattern Anal. 2001;23:228-33.
12. Team TRDC. R: A Language and Environment for Statistical Computing. 2010.
13. Fawcett T. An introduction to ROC analysis. Pattern Recogn Lett. 2006;27:861-74.
14. Bolin FP, Preuss LE, Taylor RC, Ference RJ. Refractive index of some mammalian tissues using a fiber optic cladding method. Appl Opt. 1989;28:2297-303.
15. Tearney GJ, Brezinski ME, Southern JF, Bouma BE, Hee MR, Fujimoto JG. Determination of the refractive index of highly scattering human tissue by optical coherence tomography. Opt Lett. 1995;20:2258.
16. Alberts B, Johnson A, Lewis J, Walter P, Raff M, Roberts K. Molecular Biology of the Cell 4th Edition: International Student Edition. Routledge; 2002.
17. Palade GE. An electron microscope study of the mitochondrial structure. J Histochem Cytochem. 1953;1:188-211.
18. Maier JS, Walker SA, Fantini S, Franceschini MA, Gratton E. Possible correlation between blood glucose concentration and the reduced scattering coefficient of tissues in the near infrared. Opt Lett. 1994;19:2062-4.
19. Brunsting A, Mullaney PF. Differential light scattering from spherical mammalian cells. Biophys J. 1974;14:439-53.
20. Liu H, Beauvoit B, Kimura M, Chance B. Dependence of tissue optical properties on solute-induced changes in refractive index and osmolarity. J Biomed Opt. 1996;1:200-11.
21. Drezek R, Dunn A, Richards-Kortum R. Light scattering from cells: finite-difference time-domain simulations and goniometric measurements. Appl Opt. 1999;38:3651-61.
22. Liang XJ, Liu AQ, Lim CS, Ayi TC, Yap PH. Determining refractive index of single living cell using an integrated microchip. Sensors and Actuators a-Physical. 2007;133:349-54.
23. Videla FA, Schinca DC, Scaffardi LB. Sizing particles by backscattering spectroscopy and Fourier analysis. SPIE; 2006.
24. Keshtkar A. Application of Electrical Impedance Spectroscopy in Bladder Cancer Screening. Iran J Med Phys. 2013;10:1-21.
25. Chauveau N, Hamzaoui L, Rochaix P, Rigaud B, Voigt JJ, Morucci JP. Ex vivo discrimination between normal and pathological tissues in human breast surgical biopsies using bioimpedance spectroscopy. Ann NY Acad Sci. 1999;873:42-50.
26. Surowiec AJ, Stuchly SS, Barr JB, Swarup A. Dielectric properties of breast carcinoma and the surrounding tissues. IEEE Trans Biomed Eng. 1988;35:257-63.
27. Fricke H, Morse S. The Electric Capacity of Tumors of the Breast. J Cancer Res. 1926;10:340-76.
28. Faisy C, Rabbat A, Kouchakji B, Laaban JP. Bioelectrical impedance analysis in estimating nutritional status and outcome of patients with chronic obstructive pulmonary disease and acute respiratory failure. Intensive Care Med. 2000;26:518-25.
29. Ott M, Fischer H, Polat H, Helm EB, Frenz M, Caspary WF, et al. Bioelectrical impedance analysis as a predictor of survival in patients with human immunodeficiency virus infection. J Acquir Immune Defic Syndr Hum Retrovirol. 1995;9:20-5.
30. Schwenk A, Ward LC, Elia M, Scott GM. Bioelectrical impedance analysis predicts outcome in patients with suspected bacteremia. Infection. 1998;26:277-82.
31. Norman K, Stobaus N, Zocher D, Bosy-Westphal A, Szramek A, Scheufele R, et al. Cutoff percentiles of bioelectrical phase angle predict functionality, quality of life, and mortality in patients with cancer. Am J Clin Nutr. 2010;92:612-9.
32. Abdul S, Brown BH, Milnes P, Tidy JA. The use of electrical impedance spectroscopy in the detection of cervical intraepithelial neoplasia. Int J Gynecol Cancer. 2006;16:1823-32.
33. Halter RJ, Schned AR, Heaney JA, Hartov A. Passive bioelectrical properties for assessing high- and low-grade prostate adenocarcinoma. Prostate. 2011;71:1759-67.

This paper has been checked for language accuracy by JOSAM editors.
The National Library of Medicine (NLM) citation style guide has been used in this paper.

Suggested citation: Patrias K. Citing medicine: the NLM style guide for authors, editors, and publishers [Internet]. 2nd ed. Wendling DL, technical editor. Bethesda (MD): National Library of Medicine (US); 2007-[updated 2015 Oct 2; cited Year Month Day]. Available from: http://www.nlm.nih.gov/citingmedicine